Bull. Mater. Sci. (2019) 42:135
https://doi.org/10.1007/s12034-019-1790-8

Synthesis, structural and optical properties of $K_{0.5}Na_{0.5}NbO_3$ thin films prepared by spin coating route

SHAMMI KUMAR* and **NAGESH THAKUR**
Department of Physics, Himachal Pradesh University, Shimla 171005, India
*Author for correspondence (shammirathor18@gmail.com)

MS received 12 July 2018; accepted 8 December 2018; published online 29 April 2019

Abstract. In this paper, lead-free sodium potassium niobate thin films have been prepared by using a chemical solution deposition-based spin coating route. The effect of different anealing temperatures on structural and optical properties has been studied. The phase analysis of thin films was investigated by using X-ray diffraction analysis. The microstructure and surface roughnes of thin films were studied by using atomic force microscopy. Raman spectroscopy analysis revealed that increase in annealing temperature gives rise to better crystallinity and perovskite phase. Optical parameter of thin films has been studied by using reflectance spectroscopy at room temperature. Photoluminescence analysis has been conducted by using an exciting wavelength of 300 nm at room temperature.

Keywords. Sol–gel route; thin-film; Raman spectra; optical band; photoluminescence.

1. Introduction

Lead (Pb)-free piezoelectric materials are in current demand because of the toxicity of lead-based piezoelectric materials, such as lead zirconium titanate (PZT), PLZT, PMN, etc. Now, the market for the electronic industry is mainly dominated by PZT materials because of their outstanding piezoelectric and ferroelectric properties [1,2]. Lead is a heavy metal and a main constituent of PZT materials because it contains more than 60% lead by weight. But due to toxic and volatile nature of lead oxide (PbO) during thermal heat treatment, it causes numerous health hazards to living beings and pollutes the environment [3]. Thus, many researchers all over the world are looking for an alternative material for PZTs which could replace them from the electronic industry. Among all lead-free piezoelectric materials, i.e., barium titanate (BT), NBT, KBT, $KNbO_3$, $NaNbO_3$, etc. having an ABO_3 perovskite structure, only sodium potassium niobate (KNN) is considered as a hopeful candidate because of its high Curie temperature and admirable electromechanical properties [4,5]. After the discovery of lead-free KNN-based ceramics, they have attracted much attention as alternative piezoelectric materials due to its high piezoelectric coefficient comparable to that of PZT ceramics [3]. KNN is basically a solid solution of potassium niobate ($KNbO_3$) and sodium niobate ($NaNbO_3$) having morphotropic phase boundary at 50:50 [6]. In the last few decades, there has been increasing demand for thin films due to their short power consumption rate, appropriateness for miniaturization and module integration. They are widely used in MEMS, memory storage devices, sensors, actuators, transducers and electro-optic devices [7,8].

KNN thin films have expected greater attention because of its bulk ceramic ingredient which has admirable electrical properties. KNN thin films have been synthesized by various methods i.e., pulsed laser deposition [9], aerosol deposition [10], metal organic chemical vapour deposition [11], thermal evaporation, chemical solution deposition (CSD) [12], RF sputtering [13], etc. But in the present work, we have chosen a CSD-based sol–gel route due to its simplicity, low temperature production rate, higher homogeneity in the molecular stage, stoichiometry management, higher interdiffusion of cations and cost effectiveness as compared to physical methods i.e., a solid state reaction route which often desires high vacuum conditions. A spin coating method has several steps which include solution synthesis, coating on substrate, rotation, drying, pyrolysis and annealing processes. However, it is a tedious task to obtain high-quality KNN thin films because of the volatile nature of alkali metals (Na, K) at a higher annealing temperature. The volatility of K_2O and Na_2O in KNN thin films strongly affects their structural optical and electrical properties, such as secondary phases, crystal defects, large leakage current density, low impedance, high dielectric loss and unsaturated polarization, etc. [14,15]. Hence, to make practical use of lead-free KNN thin films, it is essential to first investigate its structural and optical properties.

The present paper investigated the phase, crystalline structure and surface morphology of KNN thin films deposited on a $Pt/SiO_2/Si$ substrate at different annealing temperatures by using a spin coating route. The effect of conventional annealing temperature on optical and photoluminescence (PL) spectra has been studied at room temperature.

2. Experimental

KNN precursor solution was prepared by using a novel CSD-based sol–gel route. High purity salts like sodium acetate (>99), potassium acetate (>99) and niobium pentaethoxide (>99) were used as starting chemical reagents. These initial chemical reagents were dissolved in 2-methoxyethanol acting as a solvent according to preferred composition $K_{0.5}Na_{0.5}NbO_3$ and acetylacetone was used as a chelating agent. The prepared solution was stirred and refluxed for 4 h at a refluxed temperature of 90°C. Then, KNN solution was kept at room temperature for 48 h to obtain a clear, stable and homogeneous solution.

KNN thin films are formed by using a spin coating system for conducting platinum substrates (Pt). First, all substrates were washed with distilled water and ethanol to remove impurities present on their surfaces. The substrates were dried for 2 min at room temperature. A drop of KNN solution was taken with the help of a dropper and deposited on the surface of the substrate. The spin coating system was operated at a speed of 4000 rotations per min for 30 s. Then, the thin film was dried at 100°C for 2 min and further pyrolysed it at 450°C for 5 min. Repeat the above steps four times to obtain the desired thickness of the thin film and finally thin films were annealed at 700°C for 2 min by using a rapid annealing process. In this case, post-annealing temperature was 450°C. A similar process was repeated again with a different post-annealing temperature of 500°C for 5 min. In this case, we have annealed the thin films by gradually increasing the temperature from pyrolysis temperature of 500−750°C at a heating rate of 7°C min^{-1}. After reaching 750°C, KNN thin film was annealed for 2 min. Then, these thin films were grounded at room temperature for further structural and optical characterizations. These thin films are named as KNN700 and KNN750 according to their final annealing temperatures 700 and 750°C, respectively.

The phase determination of KNN thin films was investigated by using an X-ray diffractometer (Philips X'pert Pro) with CuKα radiation of wavelength 1.54 Å. The phonon vibrational properties were studied by using a Raman spectrometer RIRM model (RI Instruments & Innovation India). The surface morphology of the thin films was studied by using a NTEGRA AFM model (NTMDT). Optical and PL studies were performed by using a Perkin-Elmer lambda750 and Perkin Elmer-LS55 Florescence spectrometer, respectively.

3. Results and discussion

Figure 1a shows the X-ray diffraction (XRD) analysis of KNN thin films post-annealed at 450°C and finally annealed at 700°C which revealed a single phase with a pure perovskite structure. The absence of impurities and secondary phases in the XRD analysis disclosed that annealing temperature is sufficient for obtaining high-quality thin films. The Miller indices of KNN perovskite peaks are assigned according to pulsed laser deposition (PLD)-deposited KNN thin films reported by Cho [16]. The observed diffraction peaks at $2\theta = 22.35, 31.77, 45.69, 51.50$ and $57.11°$ correspond to (100), (110), (200), (210) and (211) crystal lattice planes, respectively. The intensity of the (100) plane is much higher than the (110) plane due to lower surface energy of the (100) lattice plane. Thus, (100) preferred orientation of KNN thin film is occurred. KNN700 thin film is prepared by using a rapid annealing process and showed the absence of crystal defects in thin films. Post-annealing technique is proposed to improve the degree of crystallization of thin films. In the case

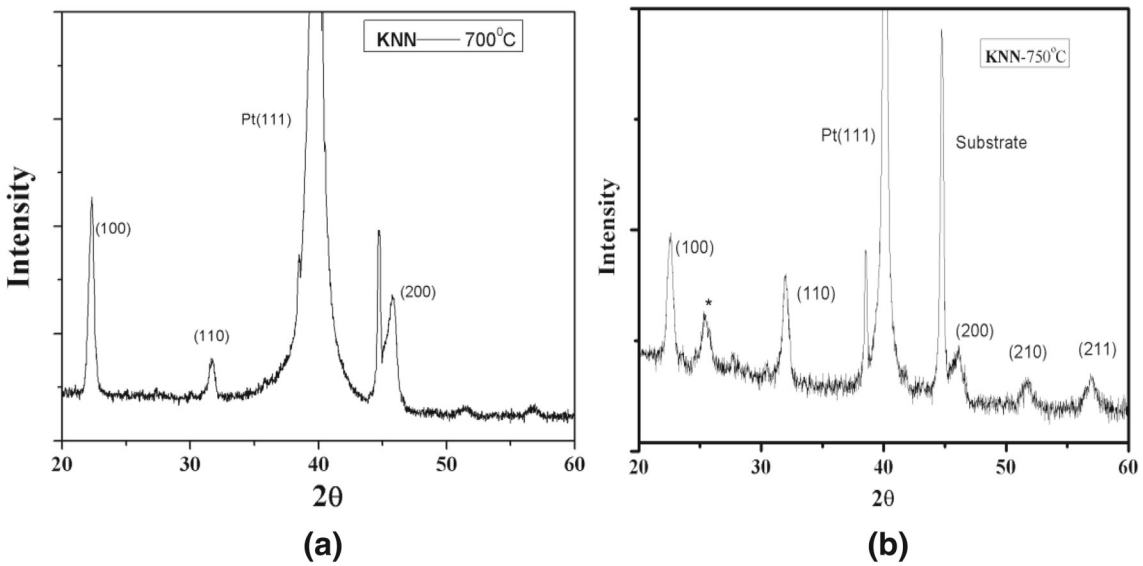

Figure 1. XRD pattern of the KNN thin films annealed at (**a**) 700 and (**b**) 750°C.

Table 1. Structural parameters of KNN thin films

Sample	Crystallite size (nm)	Lattice strain (10^{-3})	Dislocation density (10^{15})	d-spacing (100) (Å)
KNN700	20.04	9.3	2.49	3.97444
KNN750	21.03	8.8	2.26	3.94020

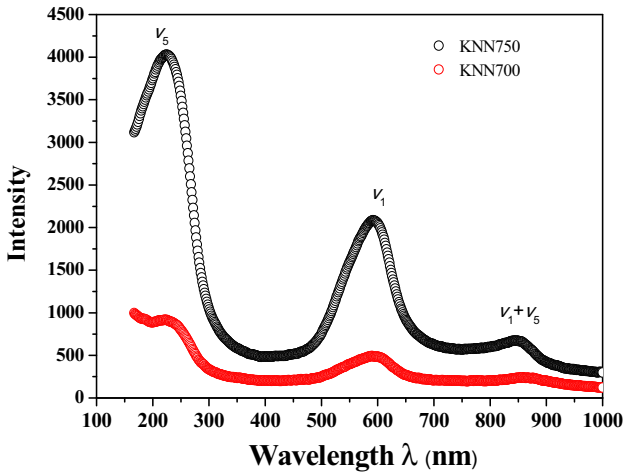

Figure 2. Raman spectra of KNN thin films annealed at 700 and 750°C.

of sol–gel route, post-annealing temperature is a significant factor because crystallinity and surface morphology of thin films are basically affected by the volatilization of organic compounds during post-annealing heat treatment [15]. The peaks around 40 and 46° are corresponding to the Pt (111) and Pt (200) planes, respectively (JCPDS 04-802).

Figure 1b shows the XRD pattern of KNN thin film post-annealed at 500°C and finally annealed at 750°C. The intensity of the thin film peaks increased with increasing annealing temperature, especially, for the (110) and (200) lattice plane diffractions. The non-perovskite peak is observed at around 25°, which is indicated by * in figure 1b. This peak is assigned to the secondary phase occurred in thin film due to volatility of alkali metal ions at higher annealing temperature (750°C). The particle size of the thin films was calculated by using the Debye–Scherer formula: $D_{hkl} = K\lambda/\beta\cos\theta$, where K is a constant quantity and its value is taken as 0.9. λ is the wavelength of the incident X-ray which is equal to 1.54 Å and β is the full width at half maxima of the corresponding peaks. The average strain and dislocation density in thin films are calculated by using the Stokes–Wilson equation: $\varepsilon_{strain} = (\beta\cot\theta)/4$ and $\delta = 1/D^2$, respectively. All these structural parameters are shown in table 1.

The relative intensity (%) of KNN750 is more than that of KNN700 for the (110) planes. We have observed that processing parameters and an increase in annealing temperature leads to increase in grain size. The value of lattice parameters is calculated by using the equation: $1/d^2 = h^2/a^2 + k^2/b^2 + l^2/c^2$. We have observed that the value of lattice parameters decreased from 0.397444 nm for KNN700 to 0.394020 nm for KNN750 which is related to increase in internal stress in the thin film at lower temperature.

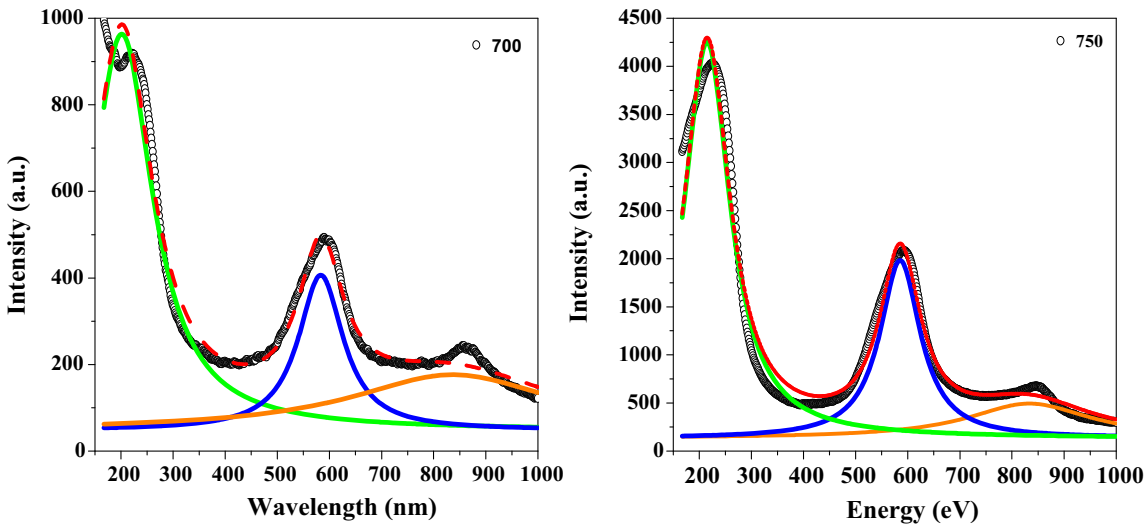

Figure 3. Fitting of Raman spectra of KNN thin films annealed at 700 and 750°C.

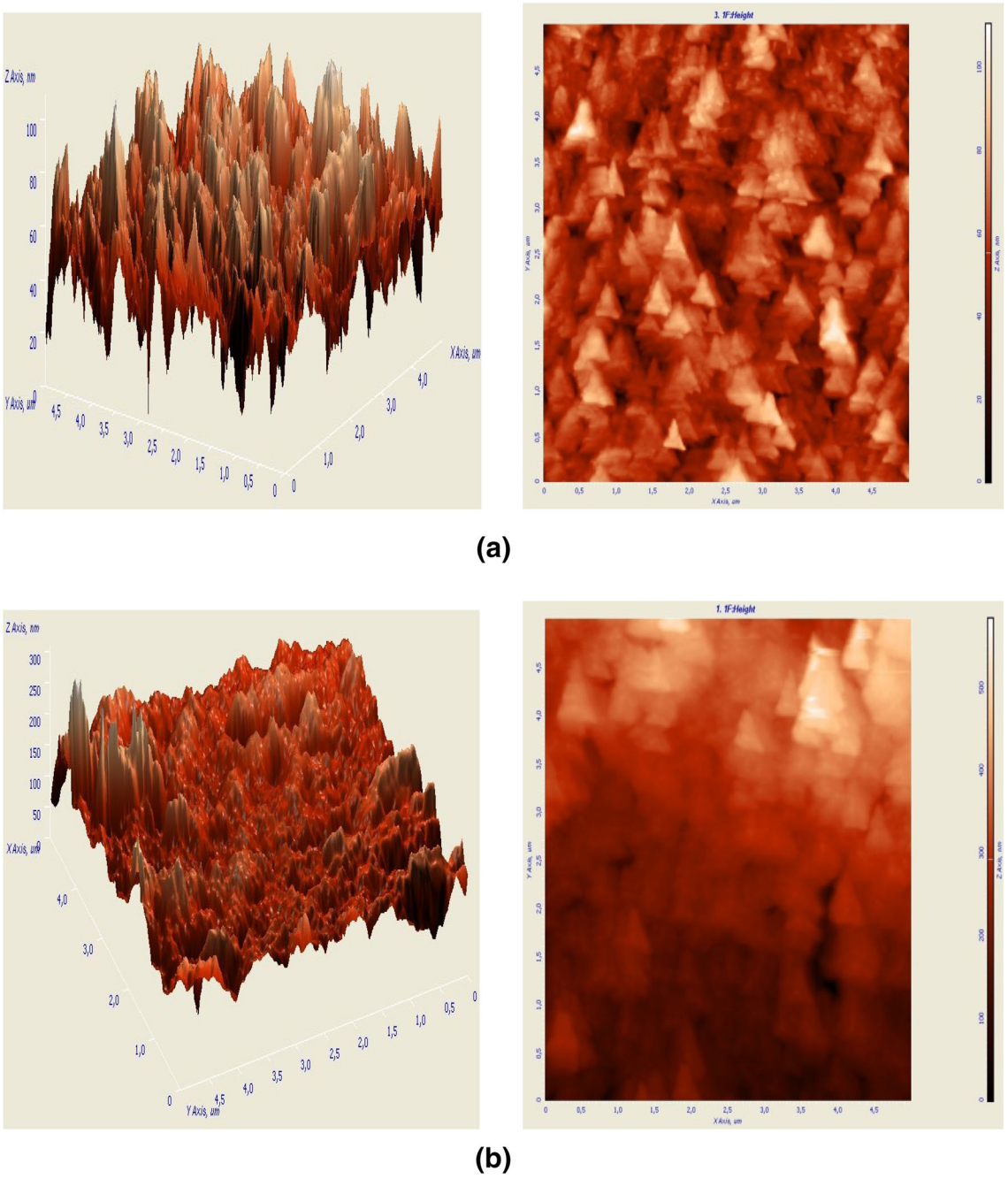

Figure 4. AFM images of KNN thin films annealed at (**a**) 700 and (**b**) 750°C.

Raman spectroscopy was conducted to study the extent of crystallization and variation in phase structure by analysing the phonon vibrational modes of thin films. Figure 2 shows the Raman spectrum of KNN thin films annealed at 700 and 750°C in the 200–1000 cm^{-1} range at room temperature. The peaks observed around 225, 594 and 851 cm^{-1} are attributed to triply degenerate symmetric O–Nb–O bending vibration $v_5(F_{2g})$, doubly degenerate symmetric O–Nb–O stretching vibration $v_1(A_g)$ and combination of $v_1 + v_5$, respectively, due to internal vibration modes of NbO_6 octahedron [17]. Figure 3 shows the fitting of Raman spectra of KNN thin films. We have observed that with the increase in annealing temperature, intensity of v_1, v_5 and $v_1 + v_5$ vibration modes noticeably increases. This increase in intensity reveals improved crystallization and perovskite phase in KNN750 as compared to KNN700 similar to the results reported in the XRD analysis (figure 1).

Figure 4 shows the 3D and 2D atomic force microscopy (AFM) images of KNN thin films annealed at 700 and 750°C. The average grain size of KNN700 thin film is 210 nm for the

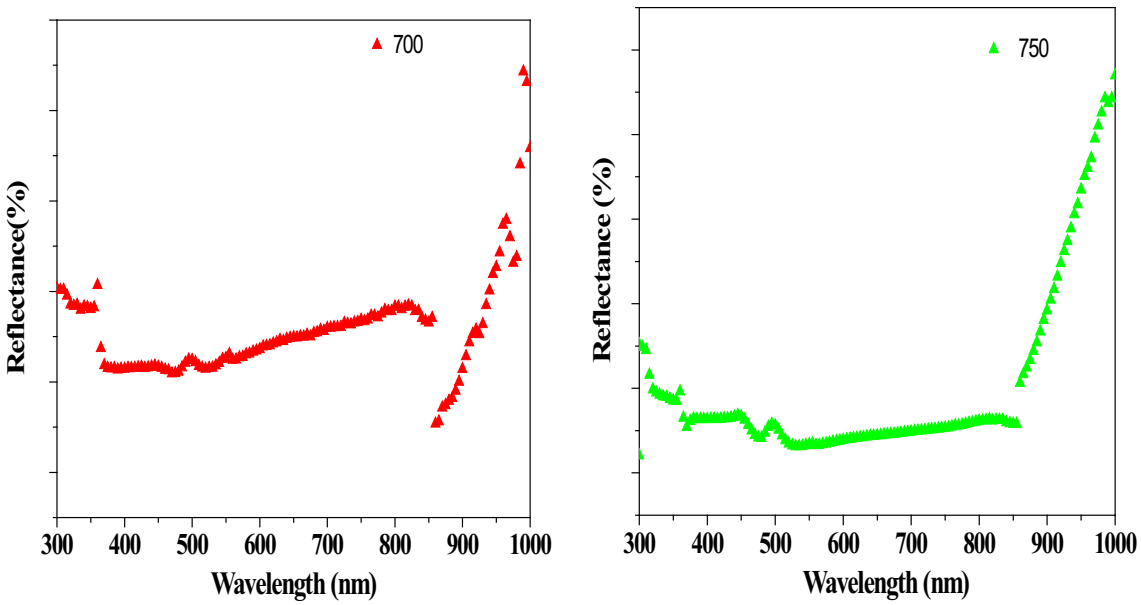

Figure 5. Reflectance spectra of KNN thin films annealed at (**a**) 700 and (**b**) 750°C.

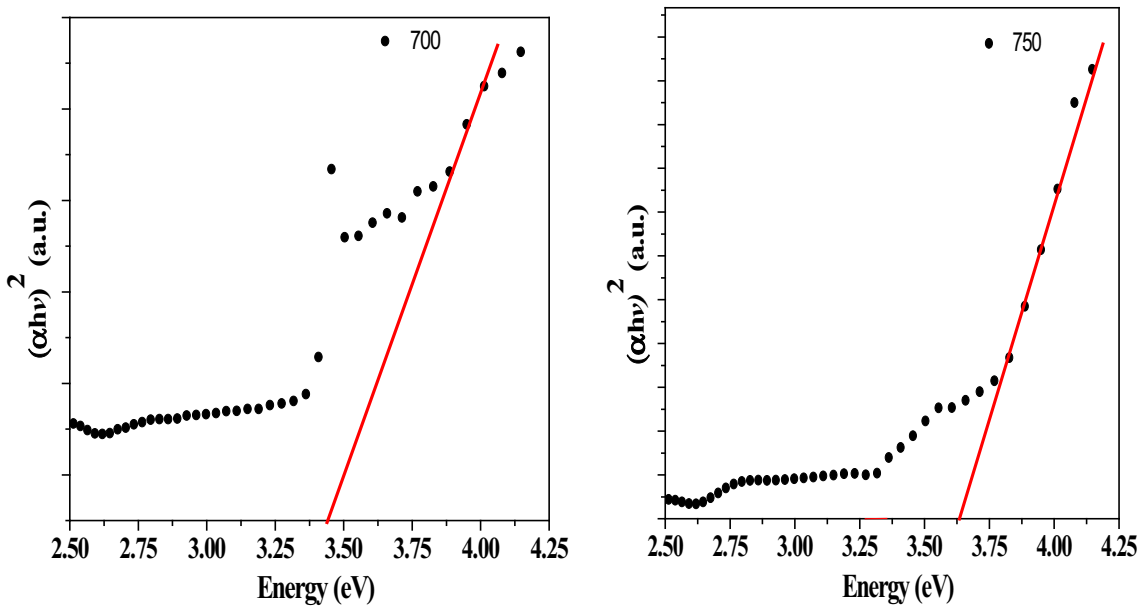

Figure 6. Plot of $(\alpha h\nu)^{1/2}$ *vs.* photon energy for KNN700 and KNN750.

sampling area of 0.0480 μm^2. Root mean square roughness and average roughness for the sampling area of 24.956 μm^2 are 13.515 and 10.679 nm, respectively. The value of area peak density and area peak to valley height are 61.267 μm^{-2} and 110.179 nm, respectively. But in the case of KNN750, average grain size increases from 210 to 259 nm. The average grain size of KNN750 thin film is 259 nm for the sampling area of 0.0737 μm^2. Root mean square roughness and average roughness are 25.309 and 18.349 nm for the sampling area of 24.956 μm^2, respectively. The value of area peak density and area peak to valley height are 36.423 μm^{-2} and 310.859 nm, respectively. This disclosed that with the increase in annealing temperature, average grain size and roughness increases. We have observed that the shape of particles starts changing from triangular to spherical shape with increase in annealing temperature. This is due to the fact that at low value of annealing temperature, interfacial surface energy of KNN thin film is high. Thus, at lower value of annealing temperature, less number of crystal grains is crystallized due to lower value of their interfacial energy. At low annealing temperature, KNN thin films did not crystallize completely which give rise to inhomogeneous surface. With rise in annealing temperature, grains become smaller and uniform which leads to transformation in their grain size and shape.

Figure 5 shows reflectance (R) spectrum of KNN700 and KNN750 thin films in the wavelength range of 300–1000 nm. The value of the optical band gap energy is calculated by exciting the valence band electrons to the conduction band. Kubelka–Munk theory is used to investigate the optical band gap energy of thin films [18,19]. According to this theory, Kubelka–Munk function, $F(R)$ is given as: $F(R) = (1 - R^2)/2R$, where R is the reflectance of the material. The value of absorption coefficient (α) is proportional to Kubelka–Munk function, $F(R)$. The relation used to find out optical band energy is: $\alpha hv = (hv - E_g)^n$, where E_g is the optical band gap, v is the incident photon frequency and n characterizes which absorption process involved in thin films, i.e., $n = 2$ for indirect band gap transitions and $n = 1/2$ for direct band gap transitions.

Figure 6 shows the graph between $(\alpha hv)^{1/2}$ *vs.* hv to determine optical band energy of KNN thin films by using the Tauc plot. The extrapolation of the linear part of variation of $(\alpha hv)^{1/2}$ with photon energy towards x-axis gives rise to the value of optical band gap energy. The values of optical band gap energies are 3.44 and 3.63 eV for KNN700 and KNN750, respectively. This revealed that optical band gap energy increases with increase in annealing temperature which shows blue shift in optical spectrum. This may be due to decrease in the number of intermediate energy levels, improved crystalline phase and microstructure of KNN thin films which is also confirmed from Raman and AFM spectra. With an increase in annealing temperature spacing between atomic particles and porosity decreases which leads to improved packing density and uniform crystal structure. Free electrons were trapped in the crystal defect states and in the grain boundaries of the KNN thin films. Higher annealing temperature favours increase in grain size which leads to decrease in density of defect states, crystal imperfections and grain boundaries.

PL study is a process which is based on spontaneous emission of light energy during optical excitation of sample at room temperature. Figure 7 shows the PL spectrum of KNN700 and KNN750 in the wavelength range of 300–600 nm at room temperature. The excited wavelength of 300 nm was used to study the PL spectra of KNN thin films. It is observed that samples revealed a broad PL emission spectrum in the UV–Visible region from 370 to 475 nm. PL spectrum has peaks at ~2.78 and 2.89 eV which are related to

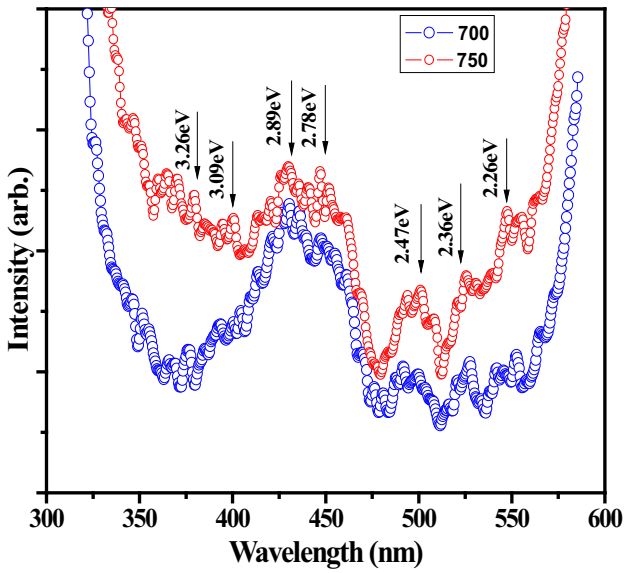

Figure 7. PL spectrum of KNN thin films annealed at (**a**) 700 and (**b**) 750°C.

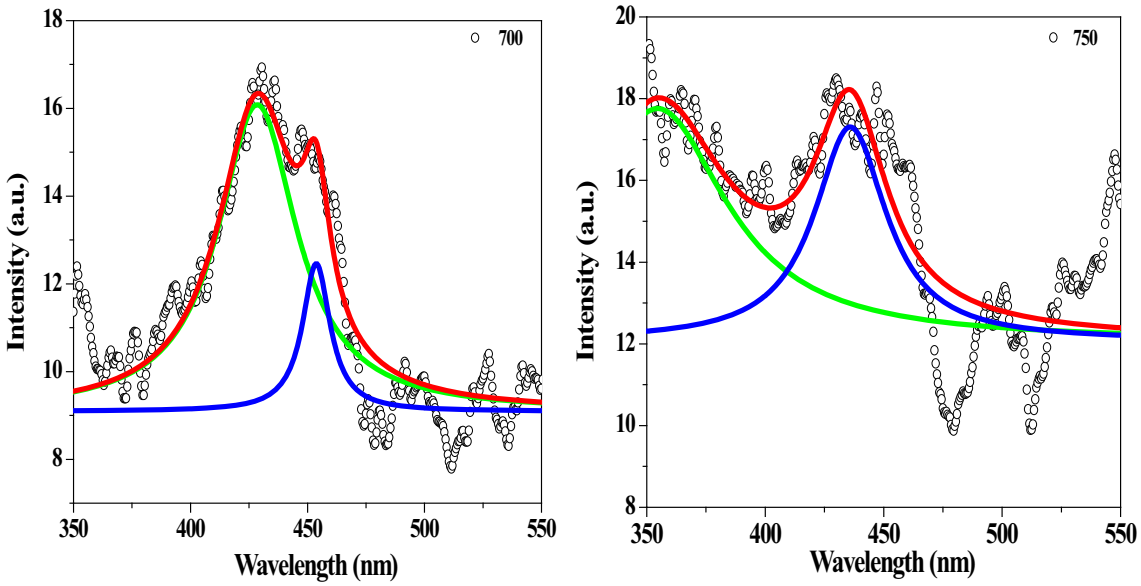

Figure 8. PL fitting of KNN700 and KNN750 thin films.

near band emission in the visible region which signifies band to band transition. The low intensity peaks observed at ∼3.26 and 3.09 eV are attributed to the ultra-violet region. The peaks at ∼2.26, 2.36 and 2.47 eV are related to the green emission band in the visible region which are associated with defect states present in thin films. The emission in the green region is usually attributed to oxygen vacancies which increase with rise in annealing temperature. Figure 8 shows the fitting of PL spectra of KNN thin films. The sharp emission band is formed which discloses that KNN thin films may be used for laser light generation. PL behaviour of KNN thin films may lead to their applications in LEDs, optical storage technology and in telecommunication fields.

4. Conclusion

KNN thin films were prepared successively by using a novel sol–gel route at different annealing temperatures. XRD and Raman spectroscopy analyses revealed that increase in annealing temperature gives rise to enhanced crystallinity and perovskite phase. AFM study showed that the KNN750 thin film has large average grain size and roughness. Optical studies showed that KNN750 has higher value of band gap energy as compared to KNN700. PL spectra have emission band in the UV–Visible region which disclosed their application in electro-optic device technology.

Acknowledgements

Shammi Kumar is thankful to the Ministry of Social Justice & Empowerment for Rajiv Gandhi National Fellowship (UGC grant no. F1-17.1/2015-16/RGNF-2015-17-SC-HIM-20898) for the financial support.

References

[1] Jaffe B, Cook W R and Jaffe H 1971 *Piezoelectric ceramics* (New York: Academic Press)
[2] Raju K and Venugopal Reddy P 2010 *Curr. Appl. Phys.* **10** 31
[3] Saito Y, Takao H and Tani T 2004 *Nature* **432** 84
[4] Yan X, Ren W and Wu X Q 2010 *J. Alloys Compd*. **508** 129
[5] Wang Y L, Lu Y Q and Wu M J 2012 *Ceram. Int.* **38** S295
[6] Egerton L and Dillon D M 1959 *J. Am. Ceram. Soc.* **42** 438
[7] Nakashima Y, Sakamoto W, Shimura T and Yogo T 2007 *Jpn. J. Appl. Phys*. **46** 6971
[8] Ostling M, Koo S M, Zetterling C M, Khartsev S and Grishin A 2004 *Thin Solid Films* **444** 469
[9] Tian A F, Ren W, Wang L Y, Chen X, Wu X, Yao Xi *et al* 2012 *Appl. Surf. Sci.* **258** 2674
[10] Ryu J, Choi J-J, Hahn B-D, Park D-S, Yoon W-H, Kim K-H *et al* 2007 *Appl. Phys. Lett.* **90** 152901
[11] Cho C-R 2002 *Mater. Lett.* **57** 781
[12] Lai F and Li F-F 2007 *J. Sol–Gel Sci. Technol.* **42** 287
[13] Blomqvist M, Koh J H, Khartsev S and Grishin A 2002 *Appl. Phys. Lett.* **81** 337
[14] Vendrell X, Raymond O, Ochoa D A, Garcia J E and Mestres L 2015 *Thin Solid Films* **577** 35
[15] Li N, Li W L, Zhang S Q and Fei W D 2011 *Thin Solid Films* **519** 5070
[16] Cho C-R and Grishin A 2000 *J. Appl. Phys.* **87** 4439
[17] Dai Y, Zhang X and Zhou G 2007 *Appl. Phys. Lett.* **90** 262903
[18] Aydõn C, Al-Hartomy O A, Al-Ghamdi A A, Al-Hazmi F, Yahia I S, Yakuphanoglu F *et al* 2012 *J. Electroceram*. **29** 155
[19] Senthilkumar V, Vickraman P and Ravikumar R 2010 *J. Sol–Gel Sci. Technol*. **53** 316